

PAPER • OPEN ACCESS

Theoretical and experimental investigations on the match between pulse tube cold fingers and linear compressors

To cite this article: Jun Tan *et al* 2015 *IOP Conf. Ser.: Mater. Sci. Eng.* **101** 012048

View the [article online](#) for updates and enhancements.

You may also like

- [Autoregressive Planet Search: Application to the *Kepler* Mission](#)
Gabriel A. Caceres, Eric D. Feigelson, G. Jogesh Babu et al.
- [Structure of the simple harmonic-repulsive system in liquid and glassy states studied by the triple correlation function](#)
V A Levashov, R E Ryltsev and N M Chitchekatchev
- [A Study of Two Periodogram Algorithms for Improving the Detection of Small Transiting Planets](#)
Yash Gondhalekar, Eric D. Feigelson, Gabriel A. Caceres et al.



ECS
The
Electrochemical
Society
Advancing solid state &
electrochemical science & technology

DISCOVER
how sustainability
intersects with
electrochemistry & solid
state science research

Theoretical and experimental investigations on the match between pulse tube cold fingers and linear compressors

Jun Tan ^{1,2}, Haizheng Dang ¹, Lei Zhang ^{1,2}

¹ National Laboratory for Infrared Physics, Shanghai Institute of Technical Physics, Chinese Academy of Sciences, No. 500 Yutian Road, Shanghai, China

² University of Chinese Academy of Sciences, No.19A Yuquan Road, Beijing, China

E-mail: tan_zhun@163.com

Abstract. The match between the cold finger and the linear compressor of the Stirling-type pulse tube cryocooler plays a vital role in optimizing the compressor efficiency and in improving the cold finger cooling performance. To reveal the match mechanism between the linear compressor and pulse tube cold finger (PTCF), detailed analyses have been made to understand the interactions between them. Based on the theoretical investigations, both of the design method of the PTCF to match the given linear compressor and a reverse method of the linear compressor to match the given PTCF have been proposed. In order to verify the validity of these theories and methods, actual PTCF and linear compressor are developed to match the existing linear compressor and PTCF, respectively. The experimental results show good agreements with the simulated ones.

1. Introduction

The Stirling-type pulse tube cryocooler (SPTC) has a wide variety of important applications in civil, aerospace and military defense fields [1–2]. Generally, a SPTC can be divided into two parts: one is the linear compressor and the other named here as the pulse tube cold finger (PTCF) including all of the remaining components. The optimal match between the PTCF and the linear compressor of the SPTC plays a vital role in optimizing the compressor efficiency and in improving the cold finger cooling performance. Several researchers had made some relevant studies on the match. For example, Heun et al. [3] carried out the investigation of gas effects on the resonance characteristics of the Stirling cycle cryocooler. Dynamic interactions between the mechanical system and the working fluid were studied and their experiments explored the effect of working fluid characteristics on the mechanical response and the effect of cryogenic temperature on the motor current and piston amplitude. Wakeland [4] investigated some issues involved in matching linear compressors to thermoacoustics cryocoolers. The results indicated that matching the acoustic load to the optimum mechanical load for the particular compressor could be used to maximize the compressor efficiency or the input power. Based on the study of Wakeland [4], Swift [5] investigated the parameters which would affect the compressor efficiency and acquired the relation between the cooler acoustic impedance and the efficiency. However, both studies made by Wakeland [4] and Swift [5] treated the whole cold finger as an acoustic impedance, whereas investigations on the impedances of the specific components of the cold finger were not made. Ko and Jeong [6] studied the dynamic behavior of the linear compressor in a SPTC and found that, the dynamic behavior of the piston in the linear compressor was directly influenced by the load condition and the flow impedance of the inertance tube



would affect the dynamic response of the piston as well as the cooling performance. Although the analyses considering the dynamics of the linear compressor and the thermo-hydraulics of the SPTC were made and a new design approach for better cooling performance was proposed, further studies on the method have not been reported.

As shown in the above literature survey, although previous studies gave some explanations or suggestions on the match between the linear compressor and the PTCF, many questions are still to be solved. For example, once the optimal acoustic impedance to match the existing linear compressor is known, how does one get or design the PTCF with the needed acoustic impedance? Few investigations have been carried out to reveal the influences of the parameters of the linear compressor on the cooling performance when matched to a PTCF. On the other hand, for an existing PTCF, specific investigations have also seldom been made to design the optimal linear compressor to match it. In order to develop high performance SPTCs for practical applications, it is necessary to study these problems thoroughly and give a clear explanation of the match mechanism.

In this paper, systematic theoretical investigations including the match of the PTCF for a given linear compressor and the reversal match of the linear compressor for a given PTCF have been made to reveal the interactions between them. Furthermore, a design method of the PTCF to achieve the optimal matching for the given linear compressor will be proposed, which is based on the electrical circuit analogy (ECA) model considering the influence of every component of the PTCF. A design method of the linear compressor to achieve the optimal matching for the given PTCF will be put forward as well. Specific experimental investigations will be carried out to verify the validity of the match theory and design methods.

2. Theoretical analyses

FIGURE 1 shows a schematic of a SPTC with a dual-opposed linear compressor as drive unit. The PTCF consists of an aftercooler, a regenerator, a cold heat exchanger, a pulse tube, a hot heat exchanger, an inertance tube and a reservoir. Through the connecting tube, the PTCF is connected to the linear compressor.

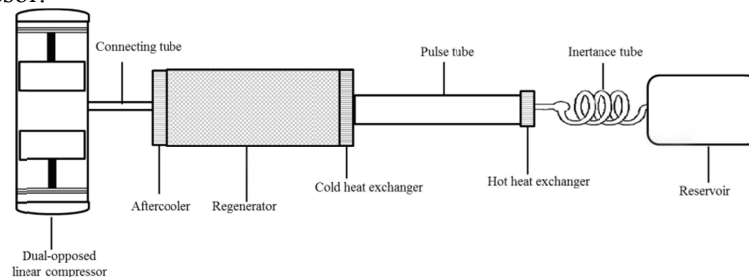


Figure 1. Schematic of a SPTC with a dual-opposed linear compressor.

The most important governing equations of the linear compressor are the force balance and the voltage potential balance of the motor. To simplify the analysis, oscillations in the linear compressor and the PTCF are all assumed to be one-dimensional and sinusoidal, and the influences of the back pressure in the linear compressor are neglected. For each motor, the governing equations can be written as Eqs. (1) and (2) [7]:

$$LBi(t) = m \frac{d^2x(t)}{dt} + b \frac{dx(t)}{dt} + k_x x(t) + \xi p(t) A_p \quad (1)$$

$$V(t) = L_e \frac{di(t)}{dt} + R_e i(t) + BL\dot{x} \quad (2)$$

Meanwhile, the displacement of the piston can be expressed in Eq. (3) as a reference point.

$$x(t) = X \sin(\omega t) \quad (3)$$

where L is the coil length in the magnetic field, B is the intensity of the magnetic field, $i(t)$ is the motor current, m is the mass of moving part, $x(t)$ is the displacement of the piston, b is the mechanical damp coefficient, k_x is the axial stiffness of the flexure springs, ξ is the pressure correction coefficient for the

dual-opposed configuration, A_p is the piston surface area, $V(t)$ is the motor voltage, L_e is the coil inductance, R_e is the coil resistance, X is the amplitude of the piston and ω is the angular frequency. Through Eqs. (1), (2) and (3), the relations between the linear compressor and the PTCF are established. Specific analyses with these equations will be carried out in the next section.

2.1. Theoretical analyses and design method of the PTCF to match the given linear compressor

According to the ECA model of the SPTC proposed by Tan and Dang [8], each part of the PTCF can be analogous to the combination of the basic fluid elements like resistance, inertance and compliance, and the whole PTCF can be analogous to an AC electrical circuit. Among the components of the PTCF, the pulse tube and the reservoir can be regarded as compliance, and thus the dynamic pressures in them are constant. The aftercooler, cold heat exchanger and hot heat exchanger are used to provide heat exchange among the working gas, the solid wall and the environment, and they should be kept at steady temperatures, respectively. In the ECA model, their impedances are all the combinations of the resistance, inertance and compliance. For the regenerator, temperature gradient will introduce a controlled source term, which will affect the volume flow rate together with the compliance. For the inertance tube, according to the ECA theory [8], the variation of volume flow rate caused by the compliance is related to the local pressure, and the pressure change caused by the inertance impedance and resistance one is related to the local volume flow rate. Hence, the total impedance of the inertance tube is the combination of the three kinds of impedances. The equivalent electrical circuit of the whole PTCF can be summarized as shown in FIGURE 2.

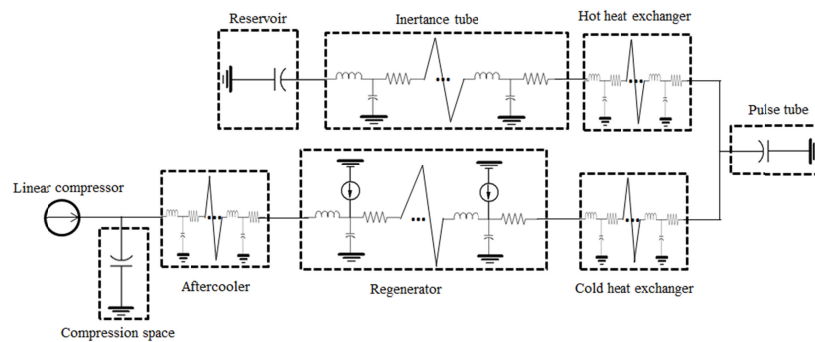


Figure 2. Equivalent electrical circuit of the SPTC.

Based on the analyses above, the PTCF can be designed and optimized by adjusting the dimensions of each component step by step. The specific design flow chart can be summarized as shown in FIGURE 3. Once the dimensions of the PTCF components are known, the specific pressure, volume flow rate and the impedance at the inlet of the PTCF can be calculated.

2.2. Theoretical analyses and design method of the linear compressor to match the given PTCF

Based on the similar approaches proposed by Wakeland [4] and the above equations, further relations between the parameters of the linear compressor and the PTCF can be re-deduced as follows. For the dual-opposed linear compressor, the motor current can be expressed as Eq. (4), and the efficiency that the electric input power converts to the PV power at the inlet of the PTCF can be written as Eq. (5).

$$i(t) = \frac{X}{BL} \left[\begin{array}{l} \sin(\omega t) (k_x - m\omega^2 - 2\xi|Z_a|\omega A_p^2 \sin\theta) \\ + \cos(\omega t) (b\omega + 2\xi|Z_a|\omega A_p^2 \cos\theta) \end{array} \right] \quad (4)$$

$$\eta = \frac{B^2 L^2 A_p^2 \left(2|Z_a| \cos\theta - \frac{\pi D_{cg} t_g^3 |Z_a|}{6\mu L_{cg}} \right)}{2|Z_a| \cos\theta A_p^2 B^2 L^2 + bB^2 L^2 + R_e A_p^4 \left[(2\xi|Z_a| \cos\theta + b/A_p^2)^2 + (2\xi|Z_a| \sin\theta + (m\omega - k_x/\omega)/A_p^2)^2 \right]} \quad (5)$$

The first term in the numerator of Eq. (5) is the PV power at the piston surface, and the second term is

the PV power loss due to the seal clearance [9]. The second term in the denominator is the mechanical damping loss of the motor, and the last term is the Joule heat due to the coil resistance.

In addition, the dynamic pressure at the piston surface provides periodic gas force on the piston. The gas force can be divided into two parts. One is out of phase with piston displacement which does work on the gas, like a gas damp, transporting the PV power to the PTCF. The other is in phase with the displacement which will not consume work, like a gas spring, forming a new mass-spring system. The resonance frequency of the linear motor becomes:

$$f_n = \frac{1}{2\pi} \sqrt{\frac{k_x - 2A_p^2 \omega \xi |Z_a| \sin \theta}{m}} \quad (6)$$

In order to achieve high performance of the linear motor, the working frequency should approximate to the resonance frequency. According to the analysis of the PTCF, the amplitude and phase angle of the impedance are also functions of working frequency. The optimal frequency becomes the solution of this transcendental equation.

According to Eqs. (4), (5) and (6), the specific of the design flow chart of the linear compressor to match the given PTCF can be summarized in FIGURE 4.

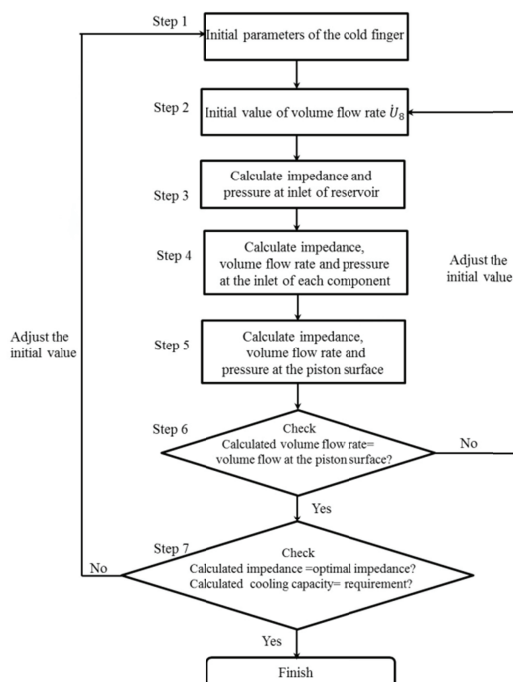


Figure 3. Flow chart of the design method of the PTCF to match the given linear compressor.

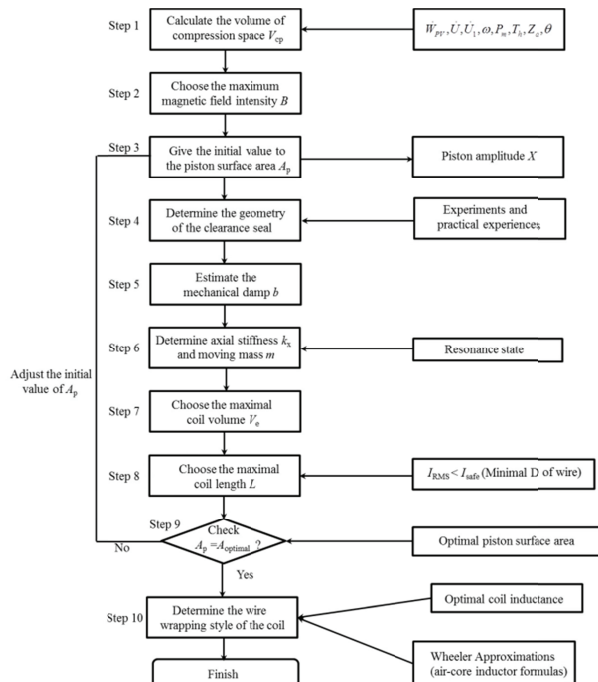


Figure 4. Flow chart of the design method of the linear compressor to match the given PTCF

And several principles can be summarized for designing the linear compressor to match the PTCF as follows:

First, considering the practical applications, the magnetic field intensity should be as high as possible, which means that the material with the largest available energy product should be chosen.

Second, based on the condition of the resonance state of the linear compressor given by Eq. (6), the optimal moving mass and the axial stiffness of the flexure springs can be achieved.

Third, when exerting no influence on the design of other parts, the volume of the motor coil in the magnetic field should be designed to be as big as possible to achieve high motor efficiency.

Fourth, keeping other variables constant, differentiating Eq. (5) with respect to term of piston area A_p and setting the result equal to zero will get the optimum value of A_p to achieve the highest motor efficiency as follows:

$$A_{optimal} = \sqrt[4]{\frac{bB^2L^2 + R_e(b^2 + (k_x / \omega - m\omega)^2)}{4R_e\xi^2|Z_a|^2}} \quad (7)$$

And fifth, based on Eqs. (2) and (4), the phase angle between the motor voltage and current can be obtained. In order to keep high efficiency, the value of the motor power factor should approximate to 1. Therefore, the value of the coil inductance can be achieved to gain the optimal power factor. Its expression is shown in Eq. (8).

$$L_{e(optimal)} = -\frac{B^2L^2(k_x - m\omega^2 - 2\xi|Z_a|\omega A_p^2 \sin \theta)}{(k_x - m\omega^2 - 2\xi|Z_a|\omega A_p^2 \sin \theta)^2 + (b\omega + 2\xi|Z_a|\omega A_p^2 \cos \theta)^2} \quad (8)$$

Once the length, the wire diameter and the coil inductance are known, the wire wrapping style can be determined according to the air-core inductor formulas based on the Wheeler approximation [10].

3. Simulations and experimental results

According to the above analyses, a new in-line PTCF will be developed to match a given linear compressor developed in the authors' laboratory, and a new dual-opposed linear compressor will be developed to match a given coaxial PTCF, to verify the validity of the above theories and design methods.

3.1. Development of the PTCF to match the given linear compressor

For the given linear compressor, the magnitudes of the magnetic field intensity B , the coil length in magnetic field L , the springs axial stiffness k_x , the moving mass m , the piston surface area A_p , the coil resistance R_e , the coil inductance L_e , the maximum piston amplitude X_{max} and mechanical damp b can all be regarded as known parameters. According to theoretical analyses, the match between its performance and the impedance of PTCF is simulated.

FIGURE 5 and FIGURE 6 show the simulated performance of the existing motor with different amplitudes and phase angles of the PTCF impedance, respectively. In FIGURE 5, the motor electric input power increases with the increase of the amplitude of PTCF impedance under different values of the impedance phase angle. With the same amplitude, there exists an optimal phase angle for the linear compressor to achieve the highest electric input power. In addition, when the impedance phase angle is smaller than zero, the motor electric input power will decrease with the decreasing phase angle. FIGURE 6 shows the variations of the motor efficiency with the increase of the amplitude of the PTCF impedance. As the mechanical loss accounts for a very small portion of the input power, the motor efficiency can be used to represent the variation of the efficiency of converting the electric input power into PV power. For each phase angle, there exists an optimal impedance to acquire the highest motor efficiency, respectively. With the decrease of the phase angle, the optimal motor efficiency increases. For this linear compressor, the simulated results show that, with negative phase angles, the highest motor efficiency can be achieved with impedance in the range of 2×10^8 Pa·s/m³ to 3×10^8 Pa·s/m³.

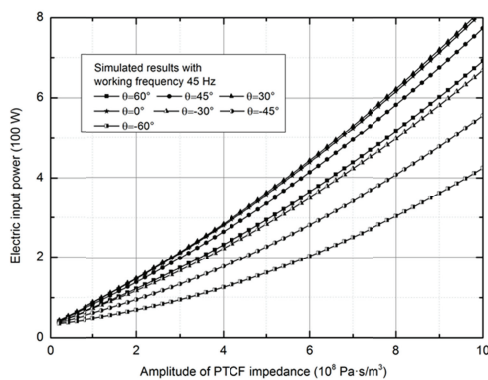


Figure 5. Simulations of the motor electric input power with different amplitudes and phase angles of the PTCF impedance.

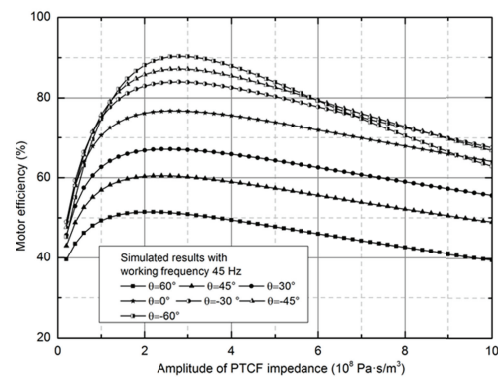


Figure 6. Simulations of the motor efficiency with different amplitudes and phase angles of the PTCF impedance.

According to the ECA model and design method of PTCF described above, a new in-line PTCF has been designed to match the existing linear compressor. As it has been discussed in the prior section, each component of the PTCF exerts an effect on the PTCF impedance and thus affects the PTCF cooling performance. In order to show this in a detailed and clear way, the influence of each component will be conducted on the developed PTCF. For example, FIGURE 7 shows simulated results of the influence of pulse tube length on the PTCF impedance and efficiency of the matched cooler. With the pulse tube length increasing from 40 mm to 140 mm, the amplitude of PTCF impedance gradually decreases, whereas an optimal cooler efficiency above 18.4% exists in the pulse tube length range of 80 mm to 100 mm. In FIGURE 8, the same variations appear with the increase of the inertance tube length. In addition, the change of the cooler efficiency is great, from 18.4% with the inertance tube length of 1 m to zero with the length of 3 m. It also shows that the inertance tube plays a vital role in influencing the cooling performance of the PTCF. Moreover, the cooling temperature also shows a great effect on the PTCF impedance and the cooler efficiency. As shown in FIGURE 9, the amplitude of PTCF impedance increases a little, whereas the cooler efficiency of Carnot achieves the maximum at 110 K, with the cooling temperature increasing from 60 K to 120 K.

The specific in-line PTCF was manufactured and assembled. The prototype was then matched with the given compressor and tested. FIGURE 10 shows the comparisons of the experimental results and the simulated results of the matched cooler cooling performance. Both of the variation tendencies of the simulated cooling capacity and the simulated efficiency of Carnot agree with the experimental results well. The matched cooler can provide 4 to 11.84 watts at cooling temperature of 80 K with the electric input power ranging from 75 W to 190 W. The average efficiency of Carnot of the cooler reaches above 17%.

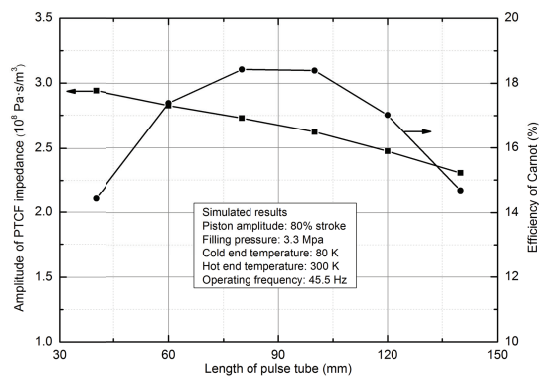


Figure 7. Influence of pulse tube length on PTCF impedance and cooling performance.

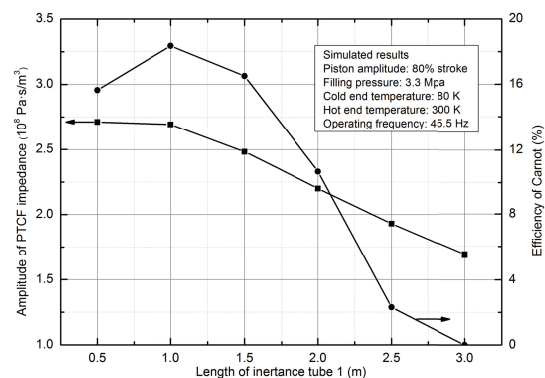


Figure 8. Influence of inertance tube length on PTCF impedance and cooling performance.

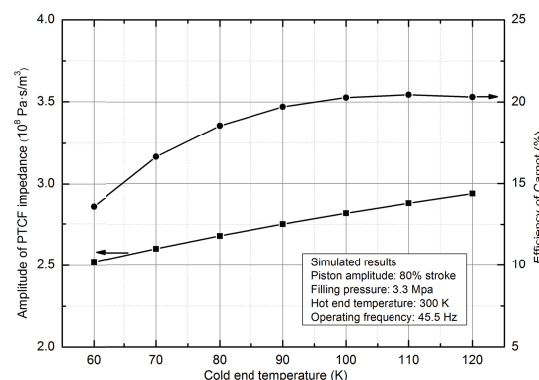


Figure 9. Influence of cooling temperature on PTCF impedance and cooling performance.

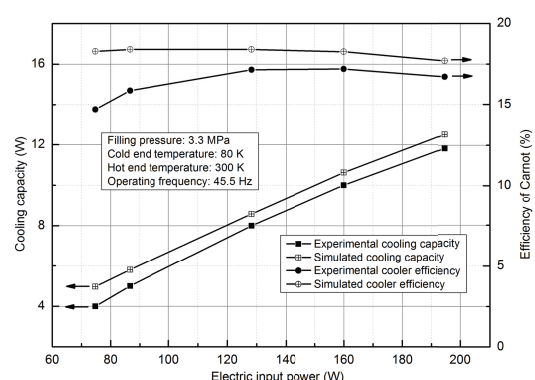


Figure 10. Comparisons between the simulated results and the experimental ones of the cooling performance.

3.2. Development of the linear compressor to match the given PTCF

For a 60 K coaxial PTCF developed in the authors' laboratory, a new linear compressor has been developed to match it. First, according to the proposed ECA model, the cooling performances of the PTCF are simulated, and 57 Hz has been achieved as the optimal working frequency. By fixing the frequency at 57 Hz and adjusting the volume flow rate at the inlet of the PTCF, the amplitude and phase angle of the impedance of the PTCF under different cooling capacity have been acquired. As shown in FIGURE 11, with the cooling capacity increasing from 2 W to 5.5 W, the amplitude of impedance has a small decrease and the phase angle has a small increase. It can be roughly considered that the amplitude and phase angle of the impedance keep constant and their values are 3.4×10^8 Pa·s/m³ and -28 degrees, respectively. FIGURE 12 and 13 show the influences of coil inductance on motor power factor, and influences of piston diameter on the cooler performance, respectively. The optimal moving mass, the axial stiffness of the flexure springs, the piston diameter and the coil inductance can be achieved accordingly.

A new linear compressor was designed by the method mentioned above, and then manufactured and assembled. The 60 K PTCF matched with the developed linear compressor was tested under different working conditions. With the working frequency of 57 Hz, the simulated cooling performance and experimental one are compared in FIGURE 14. The matched cooler achieves 2 W to 5.5 W at 60 K with the electric input power increasing from 97 W to 249 W, and 9.6% of Carnot efficiency has been realized. Tendencies of the simulated results are generally consistent with those of the experimental ones. Analyses show that the 60 K coaxial PTCF was simulated by the developed ECA model, which is mainly based on the in-line PTCF. One of the main differences between the in-line and the coaxial geometrical arrangements lies in the cold heat exchangers. The flow reverses in 180 degrees in the cold heat exchanger of the coaxial PTCF and requires more void volume, whereas the in-line counterpart does neither. These differences will lead to a deviation from the simulated result. Hence, an empirical coefficient of 0.8 has been added in the simulation to reduce this deviation. Additionally, in FIGURE 14, for the cooling capacity larger than 4 W, the difference between the experimental and simulated electric input powers becomes larger. So does the difference between the experimental and simulated cooling efficiency. The analyses give the following reasons. A larger cooling capacity needs more electric powers, and thus the current becomes larger accordingly. As the Joule heat due to the coil resistance is proportional to the square of the current, the temperature of the motor under a large electric input power increases sharply. This subsequently will result in the increases of the motor coil resistance and mechanical damp as well, both of which contribute to the motor loss. Therefore, the needed electric input power becomes larger and the cooling efficiency becomes lower accordingly.

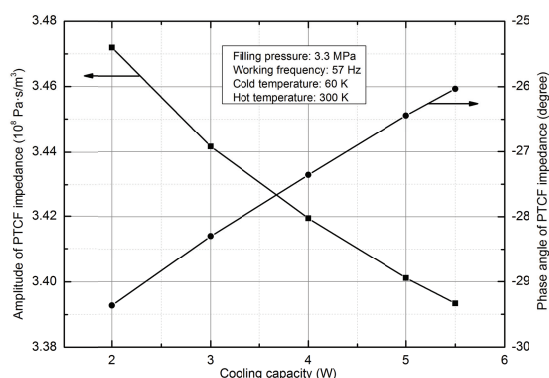


Figure 11. Simulations of amplitude and phase angle of the 60 K PTCF.

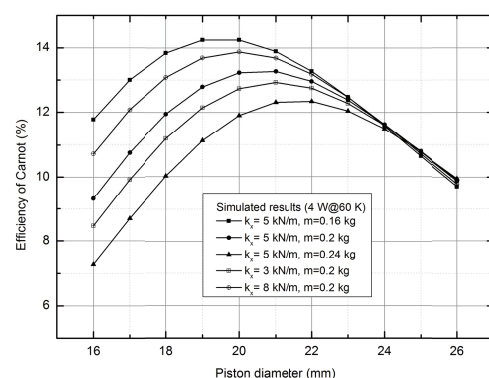


Figure 12. Cooling performance of the matched cooler with different piston diameter.

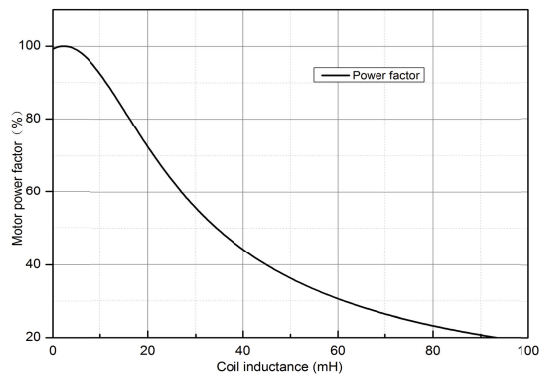


Figure 13. Influences of coil inductance on motor power factor

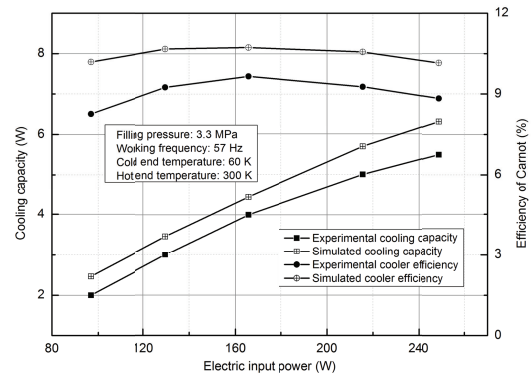


Figure 14. Comparisons of cooling performance between the simulated and the experimental ones.

4. Conclusions and discussions

The optimal match between the cold finger and the linear compressor of the SPTC plays a vital role in optimizing the compressor efficiency and in improving the cold finger cooling performance. However, the existing studies on the match only focus on achieving the optimal impedance of PTCF to match the linear compressor, or on making some specific analyses of a few components of the cold finger for the matching. In this paper, the interaction between the PTCF and the linear compressor has been analyzed in a detailed way, and the systematic investigations on the two-way matching, namely matching the PTCF for a given linear compressor and matching the linear compressor for a given PTCF have been made theoretically. Furthermore, a design method of the PTCF to achieve the optimal matching for the given linear compressor is proposed, which is based on the ECA model considering the influence of every component of the cold finger. And a design method of the linear compressor to achieve the optimal matching for the given PTCF is put forward as well. In order to verify the validity of these theories and methods, an actual PTCF and a linear compressor were developed to match the given linear compressor and PTCF, respectively. The experimental results all show good agreements with the simulated ones.

References

- [1] Radebaugh R. A review of pulse tube refrigeration. *Adv Cryog Eng* 1990; 35:1191–201.
- [2] Ross Jr RG. Aerospace coolers: a 50-year quest for long-life cryogenic cooling in space. In: Timmerhaus KD, Reed RP, editors. *Cryogenic engineering: fifty years of progress*. New York: Springer Publishers; 2006.p.225–84.
- [3] Heun MK, Collins SA, Johnson DL et al. Investigation of gas effects on cryocooler resonance characteristics. *Cryocooler* 1997; 9:421–30.
- [4] Wakeland RS. Use of electrodynamic drivers in thermoacoustic refrigerators. *J.Acoust.Soc.Am* 2000; 107(2):827–32.
- [5] Swift GW. *Thermoacoustics: A unifying perspective for some engines and refrigerators*. Sewickley (PA): Acoustical Society of America Publications, 2002.
- [6] Ko J and Jeong S. Analysis on the stirling-type pulse tube refrigerator in consideration of dynamics of linear compressor. *Cryogenics* 2008; 48:68–76.
- [7] Marquardt E, Radebaugh R, Kittel P. Design equations and scaling laws for linear compressors with flexure springs. *Cryocoolers* 1993; 7: 783–804.
- [8] Tan J and Dang HZ. An electrical circuit analogy model for analyses and optimizations of the Stirling-type pulse tube cryocooler. *Cryogenics* 2015; 71:18–29.
- [9] Reed JS, Davey G, Dadd MW et al. Compression losses in cryocoolers. *Cryocoolers* 2004; 13:209–14.
- [10] Wheeler H. Inductance formulas for circular and square coils. In: *Proceedings of IEEE* 70: 1449-50; 1982.